Liquefaction Assessment of a Loose Silty Sand Site in the 2008 M_w 6.3 Ölfus Earthquake

Fattahi Seyed Javad – Faculty of Civil and Environmental Engineering, University of Iceland, Reykjavik, Iceland, e-mail: sjf7@hi.is

Olafsdottir Elin Asta – Faculty of Civil and Environmental Engineering, University of Iceland, Reykjavik, Iceland, e-mail: elinasta@hi.is

Erlingsson Sigurdur – Faculty of Civil and Environmental Engineering, University of Iceland, Reykjavik, Iceland, e-mail: sigger@hi.is

Bessason Bjarni – Faculty of Civil and Environmental Engineering, University of Iceland, Reykjavik, Iceland, e-mail: bb@hi.is

Rupakhety Rajesh – Earthquake Engineering Research Centre, University of Iceland, Selfoss, Iceland,

e-mail: rajesh@hi.is

Abstract: Seismicity in Iceland is related to the Mid-Atlantic plate boundary and primarily consolidated in two complex fracture zones. Liquefaction was observed after the M_w 6.3 Ölfus earthquake in 2008 at the site Arnarbaeli. The site consists of a thick silty sand stratum on the banks of the estuary of the river Ölfusa, and it is located less than 10 km from the earthquake epicentre. Based on nearby time history registrations, the estimated acceleration at the site was 0.6 - 0.7g. Using a simplified method, the safety factor against liquefaction based on the equivalent linear (EL) approach has been estimated. The analysis is built on in-situ field test data (i.e., MASW, and SPT). The analysis reveals the liquefaction depth, 4.4 m. It is shown that not only the current procedure is capable of predicting the occurrence of liquefaction, but also the safety factor which is in good agreement with the observed surface evidence of liquefaction at the site.

Keywords: liquefaction hazard, MASW, SPT, South Iceland Seismic Zone, equivalent-linear site response analysis

1. Introduction

Seismicity in Iceland is related to the Mid-Atlantic plate boundary and primarily consolidated in two complex fracture zones, namely the South Iceland Seismic Zone (SISZ) and the Tjörnes Fracture Zone (TFZ). Among all the earthquakes in these areas since the year 1700, 30 earthquakes have had an estimated magnitude greater than six (Einarsson, 2008). Earthquakes of magnitude up to 7 are also possible to happen. Destructive earthquakes in Iceland tend to occur in sequences, especially within the SISZ.

The term liquefaction has been used to describe a number of related phenomena observed in loose, partially or fully saturated soils, where the soil substantially loses strength due to earthquake shaking, or other sudden changes in stress conditions. Depending on the characteristics of the soil material and the site conditions, the liquefaction phenomena can lead to sudden or incremental lateral deformations, ground oscillations, vertical settlements, and development of sand boils (Kramer, 1996; Towhata et al., 2008). This can be devastating for structures buried in or resting on liquefied soil materials. Evaluation of the liquefaction hazard of soil sites is therefore of great importance in seismically active areas.

In Iceland, soil conditions consist primarily of normally consolidated Holocene soils of basaltic origin, and postglacial sediments can be seen in a vast majority of the island

(Erlingsson, 2019). These sediments are geologically young and built up fast (Bessason and Kaynia, 2002). In other words, the local soils are often coarse silty particles including coarser grains, and they are commonly loosely compacted (Erlingsson, 2019).

Liquefaction was observed after the M_w 6.3 Ölfus earthquake in 2008 at the site Arnarbaeli. The site consists of a thick silty sand stratum on the banks of the estuary of the river Ölfusa, and it is located less than 10 km from the earthquake epicentre.

In this work, an equivalent linear (EL) site response analysis is conducted for the Arnarbaeli site, and the potential for initiation of liquefaction at the site is assessed using the simplified cyclic stress approach. A few questions are aimed to be answered in this study, which have not been addressed previously by means of a unique case study. To what extent can the simplified procedure predict the liquefaction at a volcanic sandy soil site, and how do the results compare with visual evidence? Furthermore, how do the results of the EL linear simulation affect the evaluated liquefaction hazard as compared to using an empirical formula to account for the flexibility of the soil profile?

2. Seismic activity of the South Iceland Seismic Zone

The seismic hazard in Iceland is the highest in North Europe and comparable to that in South Europe. The 475-year mean return period peak ground acceleration (*PGA*) is 0.5g in the two main seismic zones of the country. Since 2000, three destructive earthquakes have hit South Iceland, two M_w 6.5, M_w 6.4 earthquakes in June 2000 and one M_w 6.3 in May 2008 (Jonasson et al., 2021), see Figure 1. These events occurred in the middle of the South Iceland lowland, the country's largest agricultural region containing many buildings, farms, power plants, bridges, and other infrastructure. Fundamentally, although no significant building collapse, serious injury, or fatality was caused by these events, much damage occurred. A wealth of strong ground motion data and damage/loss data was collected during and after these earthquakes (Bessason and Bjarnason, 2016).

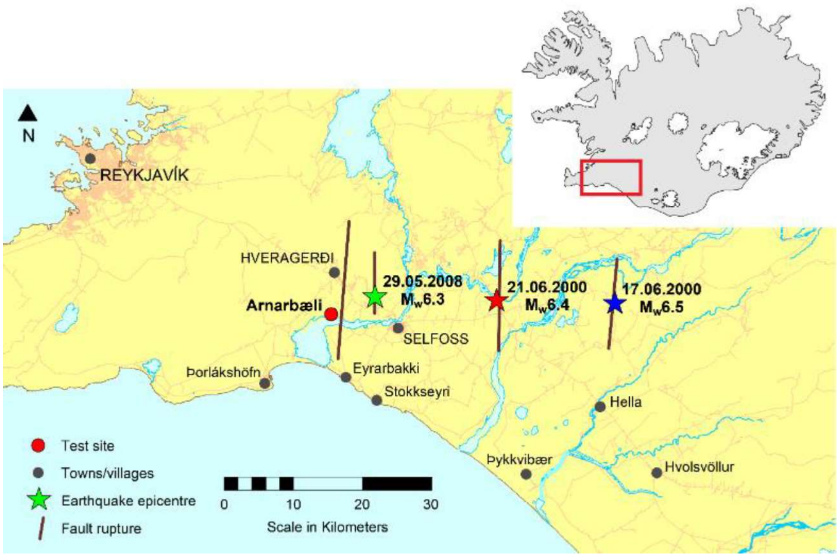

Fig. 1 - Map of South Iceland showing the epicentres and fault ruptures of the May 2008 Ölfus earthquake and the two June 2000 South Iceland earthquakes. The location of the Arnarbaeli site on the western bank of the river Ölfusa is shown by the red dot. [The map contains data from the IS 50V database of the National Land Survey of Iceland from 12/2020. Earthquake moment magnitudes and location of earthquake epicentres are from the ICEL-NMAR Earthquake Catalog (Jonasson et al., 2021).]

The epicentre of the May 2008 Ölfus earthquake was reported near the two towns, Hveragerdi and Selfoss (Figure 1). Nearly 5000 low-rise residential buildings were affected (Bessason et al., 2014). The *PGA* of the earthquake was 0.88g. Figure 2 illustrates the acceleration time history at the Selfoss town hall during the earthquake.

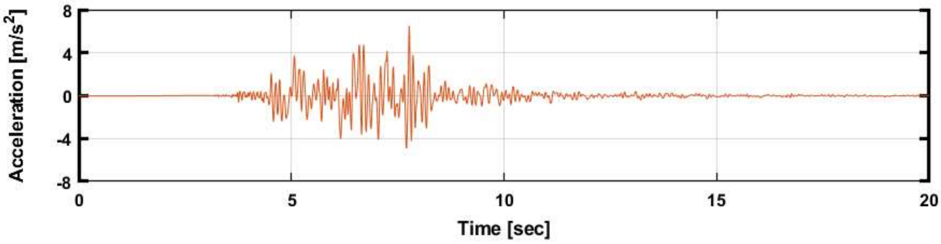

Fig. 2 – The recorded time history of acceleration (x-component) at the Selfoss town hall during the May 2008 Ölfus earthquake.

3. Site description

Liquefaction was reported after the earthquake in May 2008. The most evident surface evidence of liquefaction, such as sand boils and ground settlements, was observed at Arnarbaeli (Figure 3). The PGA at the site was estimated in the range of 0.6 to 0.7g (Green et al., 2012; Olafsdottir et al., 2019). The soil deposits at Arnarbaeli consists of a relatively homogeneous volcanic sand deposited on the west side of the estuary of the river Ölfusa.

Fig. 3 - Sand boils on the bank of the river Ölfusa close to the epicentre of the May 2008 M_w 6.3 earthquake. Figure courtesy by O. Sigurdsson.

This study has carried out a liquefaction hazard analysis for the Arnarbaeli site. Apart from the liquefaction surface evidence, the complementary reason for choosing this site was previous investigations, which contain Standard Penetration Test (SPT), shear wave velocity (V_s) measurements by the Multichannel Analysis of Surface Waves (MASW) method, and geotechnical laboratory soil characterization tests (Bessason and Erlingsson, 2011; Green et al., 2012; Olafsdottir et al., 2015, 2018, 2019; Erlingsson et al., 2022). Based on the Green et al. (2012) investigations at the Arnarbaeli site, the geotechnical properties of the basaltic sands and computed equivalent ($N_{1,60}$) blow count are presented in the following Table 1 and Figure 4, respectively. As shown in Figure 4, unfortunately, the aforementioned investigation is limited to the top 4 m of the soil.

Table 1. Geotechnical properties of the volcanic sand at Arnarbaeli (Green et al., 2012).

Specific gravity, G_s	2.84
Coefficient of uniformity, c_u	9
Coefficient of gradation, c_z	1.21
Fines content, FC	7%
USCS classification	SW-SM
Maximum void ratio, e_{max}	1.40
Minimum void ratio, e_{min}	0.647-0.694
Maximum dry unit weight, γ_{dmax}	16.4-16.9 [kN/m^3]
Minimum dry unit weight, γ_{dmin}	11.6 [kN/m^3]
Saturated unit weight at D_r = 35%, γ_{sat}	18.2 [kN/m^3]

Following this, for up to 25 m depth, the shear wave velocity of the soil layers had been measured by the MASW method. Figure 5 shows V_s over depth for the Arnarbaeli site.

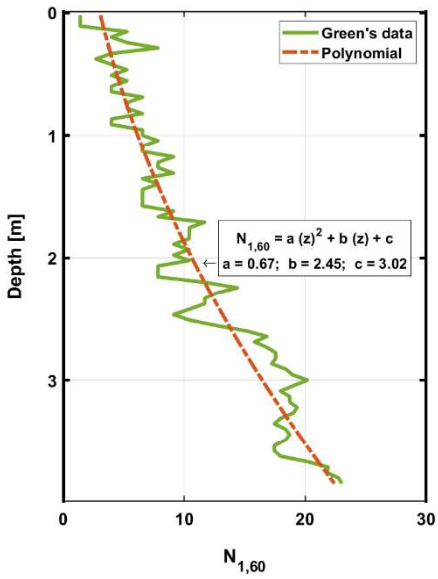

Fig. 4 - Plot of $N_{1,60}$ versus depth based on Green et al. (2012) and fitted cubic regression curve for the Arnarbaeli site. Here, z is depth in meters.

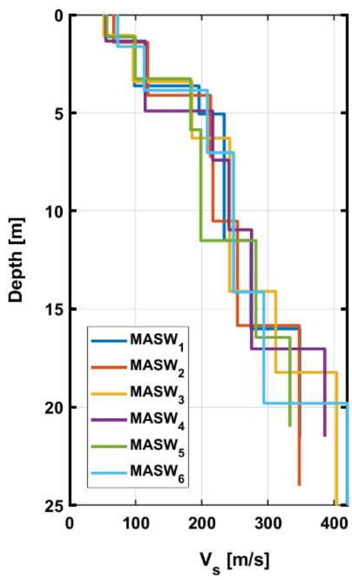

Fig. 5 – Six different MASW measurements up to 25 m depth at Arnarbaeli site.

Wair et al. (2012) summarized some SPT–V_s empirical correlation equations for various sands. Selected equations are given in Table 2. In this table, all the equations have been developed for Holocene sands.

Table 2. Selected SPT–V_s *correlations for Holocene sands.*

Study	Soil Type	Geology Age	V_s based on N_{60} [m/s]	Eq #
Piratheepan (2002)	Sand, FC<10%	Holocene	$V_s = 66.7\ (N_{1,60}^{0.25})\ (z^{0.14})$	(1)
	Sand, FC<40%	Holocene	$V_s = 72.9\ (N_{1,60}^{0.22})\ (z^{0.13})$	(2)
Wair et al. (2012)	Sand	Holocene	$V_s = 27.0\ (N_{1,60}^{0.23})\ (\sigma'^{0.25}_v)$	(3)

In these equations, z in meter, and σ'_v in kPa.

Figure 6 compares the measured shear wave velocity profiles (Figure 5) with the three SPT–V_s correlations for sandy soils given in Table 2. According to this graph, the measurements lie well within the selected equations from the literature.

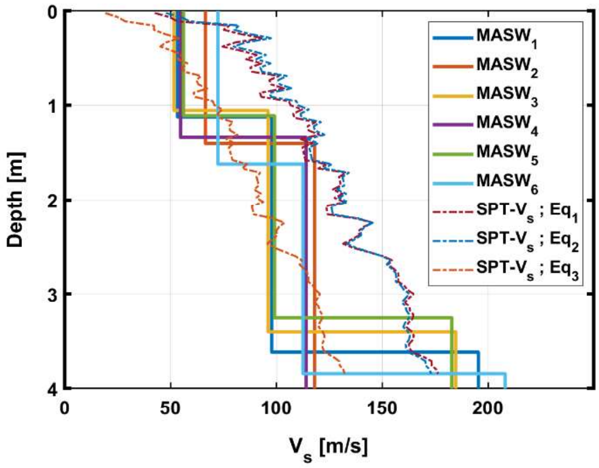

Fig. 6 – Comparison between six different MASW measurements and selected SPT–V_s relationships for the Arnarbaeli site.

4. Site response analysis

Here the input motion incident angle is considered vertical. In other words, the wave propagation's direction is perpendicular to the ground surface. The mentioned hypothesis allows 1D site response analysis in the horizontal soil layers, and the input motion propagates in only one horizontal path (Kramer, 1996). Accordingly, it is assumed that both horizontal directions are not coupled.

The Selfoss town hall time history (Figure 2) is used as an input motion in the current site response simulation. It has been applied at the bedrock bottom boundary of the soil profile. Additionally, the groundwater table is assumed to be at the ground surface.

In the EL procedure, the wave equation is solved for a linear elastic soil with constant values for the shear modulus (G) and damping (D) for each layer. For this purpose, an iterative process is utilized to determine the elastic G and D from the reduced strain, called an effective strain, reached in each layer.

In the current simulation, modulus reduction and damping curves have been derived from the empirical model introduced by Darendeli (2001). For this purpose, the dynamic parameters have been obtained based on the required variables given in Table 3 and soil type. As an example, the shear modulus reduction and material damping curves based on the Darendeli (2001) empirical modulus reduction and material damping curves are illustrated in Figure 7a.

The site response analysis provides the shear stress reduction coefficient (r_d) Figure 7b. For this purpose, the soil profile was modelled as seven layers and bedrock was estimated at a depth of 100 m. Also, the cubic regression curve is fitted to the Green et al. (2012) data ($N_{1,60}$) that has been used here for calculation $N_{1,60}$ up to 5.5 m depth, see Figure 4. For shear wave velocity of the soil profile down to 25 m depth, the $V_{s,\ average}$ of the MASW measurements, Figure 5, has been used. However, for the deeper layers, between 25 and 100 meters, anextrapolation for estimating the V_s has been utilized. The properties of the layers are presented in Table 4.

Table 3. The selected model parameters.

Model Parameter	Value
Plastic index, *PI*	0
Over-consolidation ratio, *OCR*	1.00
Exitation frequency	1.0 [Hz]
Number of cycles	10

Table 4. Soil properties.

Layer Number	Thickness [m]	V_s [m/s]
1	2	75
2	3	115
3	5	230
4	10	330
5	20	420
6	30	480
7	30	530

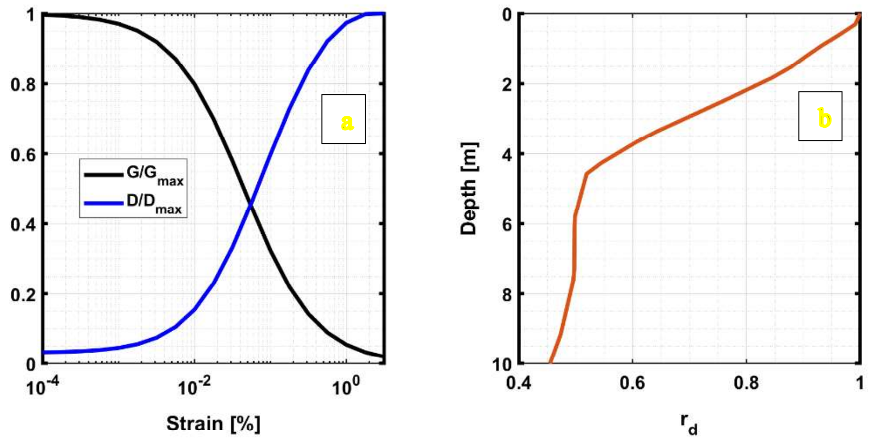

Fig. 7 – (a) According to the Darendeli (2001) empirical model, iteration procedure towards a strain compatible normalized shear modulus and material damping curves for the first soil layer has been plotted. (b) Calculated shear stress reduction coefficient based on STRATA. Only the top 10 m are shown.

5. Liquefaction hazard analysis

This paper supported the assessment of liquefaction hazard for the Arnarbaeli site by EL site response analysis through the software STRATA (Kottke and Rathje, 2009). Soil sieve analysis showed that the material is sand with FC of 6-7%, and it lies within the boundaries identified as potentially liquefiable soils (Tsuchida, 1970; Green et al., 2012).

The simplified procedure (Youd and Idriss, 2001) has been used to assess the liquefaction potential of the Arnarbaeli site. Two parameters are essential in this method, namely,

1) Cyclic Stress Ratio, *CSR*, which represents the level of cyclic loading on the soil due to the earthquake.

2) Cyclic Resistance Ratio, *CRR*, which represents soil resistance against liquefaction.

Following the procedure outlined in Andrus and Stokoe (2000), the *CSR* value is calculated through the following equation:

$$CSR = 0.65 \left(\frac{a_{max}}{g}\right)\left(\frac{\sigma_v}{\sigma'_v}\right) r_d \tag{4}$$

where a_{max} is the peak horizontal ground surface acceleration; g is the acceleration of gravity; σ'_v is the initial effective vertical (overburden) stress; σ_v is the total overburden stress, r_d is the shear stress reduction coefficient which is included to adjust for the flexibility of the soil profile.

In this study, for separating liquefied from the non-liquefied depths over the soil profile, the cyclic resistance ratio, *CRR*, is evaluated based on SPT-$N_{1,60}$ (Youd and Idriss, 2001) and scaled for a magnitude M_w 6.3 earthquake as:

$$CRR = \left(\frac{1}{34-(N_1)_{60}} + \frac{(N_1)_{60}}{135} + \frac{50}{[10(N_1)_{60}+45]^2} - \frac{1}{200}\right) \cdot MSF \tag{5}$$

This equation is valid for $(N_1)_{60} < 30$, and *MSF* is the magnitude scaling factor.

Based on the 1996 NCEER workshop (Youd and Idriss, 2001), *MSF* can be represented by the following equation:

$$MSF = \left(\frac{M_w}{7.5}\right)^{-2.56} \tag{6}$$

Where M_w is the moment magnitude.

The factor of safety (*FS*) is finally defined as:

$$FS = \frac{CRR}{CSR} \tag{7}$$

In case $FS < 1$, liquefaction can be foreseen to occur, while it is predicted not to occur when $FS > 1$.

6. Results and discussion

In this study, a simplified stress-based procedure has been utilized to predict the occurrence of liquefaction at the Arnarbaeli site. For this purpose, results obtained through an EL site response analysis in STRATA were compared with the study of Green et al. (2012). Green et al. (2012) conducted a case study comparing the observed and predicted liquefaction for the Arnarbaeli site. Following this, the simplified liquefaction evaluation procedure by means of in-situ field test data, SPT, and empirical formula for calculating r_d had been used.

The outcomes of this study show that the current procedure correctly predicts the occurrence of liquefaction. The outcomes possess good compatibility with the observed surface evidence of liquefaction at the site, Figures 8 and 3.

In Figure 8a, a liquefaction resistance curve ($N_{1,60}$ - *CRR*) is scaled based on the M_w 6.3 Ölfus earthquake. Computed equivalent ($N_{1,60}$) SPT blow count and *CSR* were plotted for reference points at a depth between the surface and down to 5.5 m depth and compared to the *CRR* value. According to the results presented in Figure 8a, liquefaction occurred down to a depth of 4.4 meters. Contrary to the investigation of Green et al. (2012), the *CSR* values are not limited to the small depth, 3.8 m. Therefore, the test site's liquefaction depth is predicted in this study.

Based on the simplified method, the factor of safety against liquefaction has been calculated and shown in Figure 8b. Accordingly, the *FS* is sketched against $N_{1,60}$ and plotted for reference points at a depth between the surface and 4.6 m. As can be seen, the *FS* increases with increasing $N_{1,60}$. Furthermore, Green et al. (2012) highlighted the over-estimation of *CSR* and consequently the relatively low factor of safety based on their investigation. The authors pointed out their findings may indicate limited applicability of the simplified procedure to evaluate the liquefaction potential for volcanic sand deposits (Green et al., 2012). However, the *FS* obtained from this study is higher than their values. In other words, it is clear that the equivalent-linear site response analysis can challenge traditional approaches.

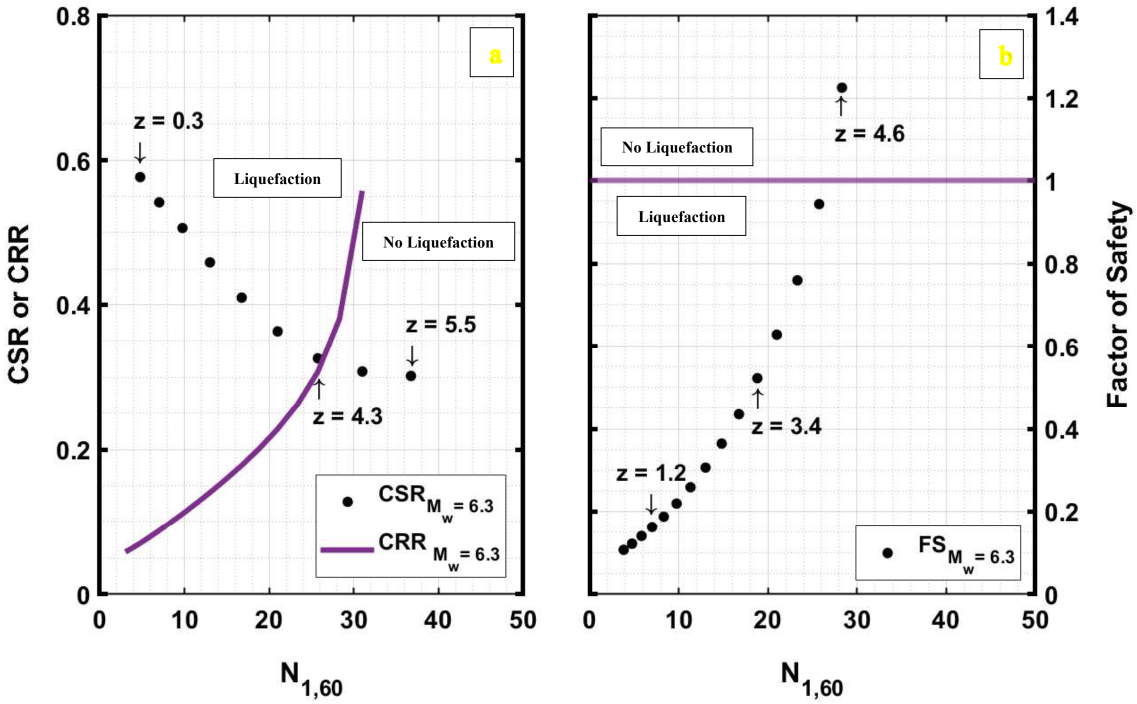

Fig. 8 - Liquefaction potential assessment in this study. (a) Liquefaction evaluation graph for the Arnarbaeli site with Green et al. (2012) data through EL site response analysis. (b) The factor of safety based on obtained data from EL site response analysis. In both figures, *z* is depth in meters.

7. Conclusions

Liquefaction was observed after the M_W 6.3 Ölfus earthquake in 2008 at the site Arnarbaeli. The site consists of a thick silty sand stratum on the banks of the estuary of the river Ölfusa, and it is located less than 10 km from the earthquake epicentre. Based on nearby time history registrations, the estimated acceleration at the Arnarbaeli site was 0.6 - 0.7g. This investigation has been based on the outcomes of in-situ field tests, namely, MASW measurements, and SPT tests at the site.

The simplified procedure, which takes advantage of EL analysis for assessing *CSR,* reveals that the liquefaction occurred at the site down to 4.4 m depth.

Based on the severity of observed liquefaction at the test site, the EL site response analysis shows more realistic results than traditional approaches based on the empirical formulas on the scope of the simplified procedure.

Future steps will include assessing the dynamic soil characteristics at the test site through advanced laboratory testing to improve the site response simulations and assessment of liquefaction potentials.

Acknowledgements

This work was supported by the Icelandic Research Fund (Rannis), Grant numbers: 206793-052 and 218149-051.

References

- Andrus, R.D., Stokoe, K.H. (2000). Liquefaction resistance of soils from shear-wave velocity. J. Geotech. Geoenvironmental Eng. 126, 1015–1025.
- Bessason, B., Bjarnason, J.O. (2016). Seismic vulnerability of low-rise residential buildings based on damage data from three earthquakes (M_w6. 5, 6.5 and 6.3). Eng. Struct. 111, 64–79.
- Bessason, B., Bjarnason, J.O., Gudmundsson, A., Solnes, J., Steedman, S. (2014). Analysis of damage data of low-rise buildings subjected to a shallow M_w6.3 earthquake. Soil Dyn. Earthq. Eng. 66, 89–101.
- Bessason, B., Erlingsson, S. (2011). Shear wave velocity in surface sediments. Jokull 61, 51–64.
- Bessason, B., Kaynia, A.M. (2002). Site amplification in lava rock on soft sediments. Soil Dyn. Earthq. Eng. 22, 525–540.
- Darendeli, M.B. (2001). Development of a new family of normalized modulus reduction and material damping curves. Doctor of philosophy dissertation. The University of Texas at Austin.
- Einarsson, P. (2008). Plate boundaries, rifts and transforms in Iceland. Jokull 58, 35–58.
- Erlingsson, S. (2019). Geotechnical challenges in Iceland, 17th European Conference on Soil Mechanics and Geotechnical Engineering, ECSMGE 2019, 1 September 2019 through 6 September 2019. International Society for Soil Mechanics and Geotechnical Engineering, Reykjavík, Iceland, pp. 27–51. https://doi.org/10.32075/17ECSMGE-2019-1109
- Erlingsson, S., Olafsdottir, E.A., Bessason, B. (2022). Soil site stiffness categorization based on MASW field testing. 20th Int. Conf. Soil Mech. Geotech. Eng. Syd. Aust.
- Green, R.A., Halldorsson, B., Kurtulus, A., Steinarsson, H., Erlendsson, O. (2012). A unique liquefaction case study from the 29 May 2008, M_w6.3 Olfus earthquake, southwest Iceland, Proceedings of the 15th World Conference on Earthquake Engineering, Lisbon, Portugal. pp. 24–28.
- Jonasson, K., Bessason, B., Helgadottir, A., Einarsson, P., Gudmundsson, G.B., Brandsdóttir, B., Vogfjörd, K.S., Jónsdóttir, K. (2021). A harmonized instrumental earthquake catalogue for Iceland and the northern Mid-Atlantic Ridge. Nat. Hazards Earth Syst. Sci. 21, 2197–2214.
- Kottke, A.R., Rathje, E.M. (2009). Technical manual for Strata. Pacific Earthquake Engineering Research Center Berkeley, California.
- Kramer, S.L. (1996). Geotechnical earthquake engineering. Pearson Education India.
- Olafsdottir, E.A., Bessason, B., Erlingsson, S. (2015). MASW for assessing liquefaction of loose sites, Proceedings of the XVI European Conference on Soil Mechanics and Geotechnical Engineering (XVI ECSMGE), Edinburgh, 13-17 September, pp. 2431-2436, https://doi.org/10.1680/ecsmge.60678.
- Olafsdottir, E.A., Bessason, B., Erlingsson, S. (2019). Application of MASW in the South Iceland Seismic Zone, Proceedings of the International Conference on Earthquake Engineering and Structural Dynamics. Springer, pp. 53–66.

- Olafsdottir, E.A., Erlingsson, S., Bessason, B. (2018). Tool for analysis of MASW field data and evaluation of shear wave velocity profiles of soils, Can. Geotech. J. 55: 217–233. https://doi.org/10.1139/cgj-2016-0302.
- Piratheepan, P. (2002). Estimating shear-wave velocity from SPT and CPT data. Master of Science thesis. Clemson University, South Carolina.
- Towhata, I., Wu, W., Borja, R.I. (2008). Geotechnical Earthquake Engineering 1. https://doi.org/10.1007/978-3-540-35783-4
- Kottke, A.R., Rathje, E.M. (2009). Technical manual for Strata. Pacific Earthquake Engineering Research Center Berkeley, California.
- Tsuchida, H. (1970). Prediction and countermeasure against the liquefaction in sand deposits, Abstract of the Seminar in the Port and Harbor Research Institute. pp. 31–333.
- Wair, B.R., DeJong, J.T., Shantz, T. (2012). Guidelines for estimation of shear wave velocity profiles. Pac. Earthq. Eng. Res. Cent. Hqrs. Univ. Calif. 1.
- Youd, T.L., Idriss, I.M. (2001). Liquefaction resistance of soils: summary report from the 1996 NCEER and 1998 NCEER/NSF workshops on evaluation of liquefaction resistance of soils. J. Geotech. Geoenvironmental Eng. 127, 297–313.